Effect of Zinc Incorporation in $CuInS_2$ Thin Films Grown by Vacuum Evaporation Method

M. Ben Rabeh*, M. Kanzari and B. Rezig
Laboratoire de Photovoltaïque et Matériaux Semi-conducteurs — ENIT BP 37
Le Belvédère 1002, Tunis, Tunisie

(Received July 28, 2008; in final form December 22, 2008)

Structural, optical and electrical properties of Zn-doped $CuInS_2$ thin films grown by double source thermal evaporation method were studied. Evaporated thin films were grown from $CuInS_2$ powder by vacuum evaporation using resistively heated tungsten boats. The element Zn was evaporated from a thermal evaporation source. The amount of the Zn source was determined to be 0–4% molecular weight compared with $CuInS_2$ source. The effects of Zn on films properties were investigated using X-ray diffraction, optical transmission and reflection spectra. The films were annealed in vacuum at 260°C for 2 h. The Zn-doped samples have band-gap energy of 1.474–1.589 eV. We found that the Zn-doped $CuInS_2$ thin films exhibit *p*-type conductivity and we predict that Zn species can be considered as suitable candidates for use as doped acceptors to fabricate $CuInS_2$-based solar cells.

PACS numbers: 68.55.ag, 78.20.Ci, 81.15.Ef, 73.61.Le

1. Introduction

Because of their high absorption coefficient of sun light and their high tolerance to the presence of defects (grain boundaries, vacancies, interstitials, etc.), ternary chalcopyrite, CI(S,Se) are becoming among the leading candidates for high efficiency and low-cost terrestrial photovoltaic devices. Indeed, polycrystalline CI(S,Se) based solar cells have achieved efficiencies of about 19% on a laboratory scale [1–3] and around 14% for module [4]. $CuInS_2$, a photoabsorbing semiconductor with a direct band gap close to 1.5 eV [5], has recently been introduced into industrial production [6]. It exhibits a high light absorbing coefficient in the visible spectral range and stability. For controlling a conduction type and obtaining a low resistivity, several impurities doped $CuInS_2$ bulks have been studied. The process can be of interest for application in $CuInS_2$-based cell design [7]. For example, the incorporation of iron during the crystal growth of $CuInS_2$ by chemical vapor transport was studied [8, 9]. Mittleman and Singh [10] investigated the electrical properties of cadmium and zinc doped $CuInS_2$ crystals grown by the Bridgman technique. Ueng and Hwang [11] concluded that in this case the crystals annealed in cadmium and zinc vapors exhibited shallow activation energies of 0.02 and 0.025 eV, respectively. In addition, they reported the results of electrical and photoluminescence measurements of phosphorus doped and zinc doped $CuInS_2$ crystals. Yamamoto and Yoshida [12] showed that *p*-type doping using the group V elements such as N, P and As increases the Madelung energy, which gives rise to instability of ionic charge distribution in *p*-type doped $CuInS_2$ crystals. The difference in the electronic structures and compensation mechanism between *n*-type Zn- and Cd-doped $CuInS_2$ crystals was investigated [13]. Sb doping of $CuInS_2$ was investigated [14] using vacuum evaporation method. A single phase Sb-doped $CuInS_2$ can be prepared by annealing above 400°C in Ar or N_2. The effect of Na doping on the properties of $CuInS_2$ thin films has been also investigated [15]. The incorporation of the doping element Sn in $CuInS_2$ was succeeded [16] by annealing the Sn-doped films in vacuum. After annealing the Sn-doped $CuInS_2$ exhibit *n*-type conductivity. In our previous paper [17], $CuInS_2$ films annealed in air atmosphere from 100 to 350°C present an irreversible *n*-type conductivity from the annealing temperature 260°C. On the other hand, it has been shown that the open circuit voltage of solar cells based on $CuInS_2$ can be enhanced via controlled doping of small amounts of zinc [18]. Therefore, we report in this paper, the structural, morphological and optical properties of the Zn-doped $CuInS_2$ thin films grown by double source thermal evaporation method.

2. Experimental procedures

2.1. Synthesis of $CuInS_2$

Stoichiometric amounts of the elements of 99.999% purity Cu, In, and S were used to prepare the initial ingot of $CuInS_2$. The mixture was sealed in vacuum in a quartz tube. In order to avoid explosions due to sulfur vapor pressure, the quartz tube was heated slowly (20°C/h). A complete homogenization could be obtained by keeping the melt at 1000°C thermal expansion of the melt on solidification was avoided. X-rays of powder analysis showed that only homogeneous $CuInS_2$ phase was present

* corresponding author; e-mail: mohamedbenrabeh@yahoo.fr

in the ingot. Crushed powder of this ingot was used as raw material for the thermal evaporation.

2.2. Film preparation

$CuInS_2$/Zn thin films were prepared by co-evaporation of the $CuInS_2$ powder and the Zn element in a high vacuum system with a base pressure of 10^{-6} Torr. Zn of 4N purity was evaporated from thermal evaporator. An open ceramic crucible was used. Zn was deposited simultaneously during the deposition of the $CuInS_2$ powder (see Fig. 1). Thermal evaporation sources were used which

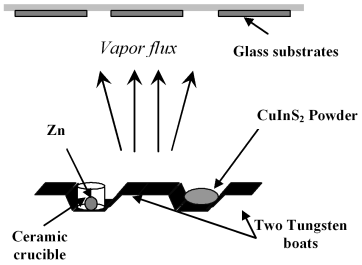

Fig. 1. A schematic drawing of the films deposition system.

can be controlled either by the crucible temperature or by the source powder. The glass substrates were not heated during the evaporation process. The amount of the Zn source was determined to be 0–4% molecular weight compared with the $CuInS_2$ alloy source. Film thickness was measured by interference fringes method [19]. Typical as-deposited films thicknesses were in the range of 580–770 nm after that the films were annealed in vacuum for 2 h at the temperature 260°C.

2.3. Characterization

The structure of the Zn-doped thin films was determined by means of X-ray diffraction (XRD) using a D8 Advance diffractometer with Cu K_α radiation ($\lambda = 1.5418$ Å). The optical characteristics were determined at normal incidence in the wavelength range 300 to 1800 nm using a Shimadzu UV/VIS-spectrophotometer. The film's thicknesses were calculated from the positions of the interference maxima and minima of reflectance spectra using a standard method. The type of conductivity of these films was determined by the hot probe method.

3. Results and discussion

3.1. XRD analysis

3.1.1. Structural properties

Figure 2 shows the results of our XRD measurements after annealing of undoped and Zn doped $CuInS_2$ thin films. Vacuum-evaporated films are usually considered to be randomly oriented polycrystalline. It was found that the zinc concentration has great effects on the formation of polycrystalline $CuInS_2$. All diagrams present

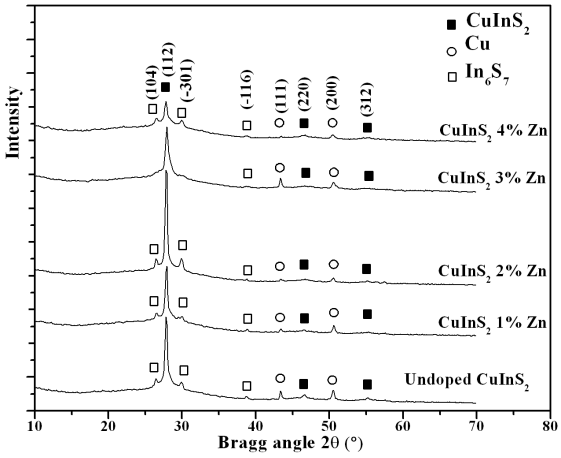

Fig. 2. X-ray diffraction patterns of undoped and Zn-doped $CuInS_2$ thin films with different Zn% molecular weight.

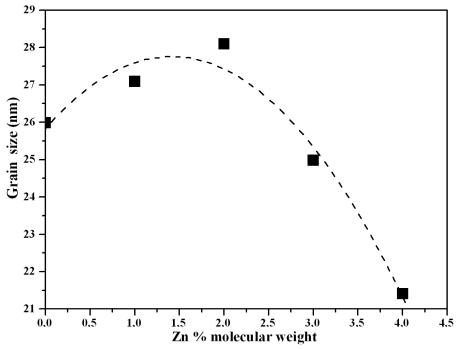

Fig. 3. Variation of the grain size of undoped and Zn-doped $CuInS_2$ thin films with different Zn% molecular weight.

peak at $2\theta = 27.9°$ assigned to the (112) reflection of the $CuInS_2$ phase and an improvement in the growth of the films was observed after annealing. It was also observed that the (112) peak intensity decreases obviously with increasing zinc concentrations, which are due to increase in the disorder part (see Fig. 2). However, few minor peaks with lower intensities identified as In_6S_7 and Cu phases were detected. The presence of the minor phases is in general attributed to a sum of internal origins obeying the thermodynamics of solid solutions, to defect chemistry and the thermal gradient which plays an important role, as described elsewhere [20]. Indeed, the additional copper phase is mainly attributed to the higher mobility of Cu^+ and its migration towards the surface layers [21].

3.1.2. Grain sizes values

The grain size along the (112) peak can be evaluated by using the Debye–Scherrer relation

$$L = \frac{0.9\lambda}{\cos(\theta_0)\Delta(2\theta)}, \tag{3.1}$$

where λ is the wavelength of the X-ray radiation used, 2θ

is the half intensity width of the peak and θ_0 — the Bragg angle. Figure 3 shows the behavior of grain size versus the Zn% molecular weight. As we can see from Fig. 3 the grain sizes are in the range 21–28 nm. The maximum value was obtained for 2 Zn% molecular weight. This result confirmed the XRD analysis which shows an improvement of the crystallinity at this Zn% of molecular weight. Probably for the lower Zn% molecular weight (0–2%) the incorporation of Zn namely in part occupying the sulfur site without affecting the structure [11] since the single source thermal evaporation method leads to $CuInS_2$ sulfur defect [22]. Therefore, the Zn in lower concentration leads to an improvement in crystallinity by occupying the sulfur sites. However, after saturation of the sulfur sites the Zn contributes to degradation in crystallinity properties.

3.2. Optical properties

3.2.1. Optical transmission and reflection spectra

The reflection and transmission spectra were recorded in the spectral wavelength range 300–1800 nm at normal incidence. Figures 4 and 5 show the reflection and transmission spectra of the Zn-doped $CuInS_2$ films after annealing, respectively. All the transmission spectra show interferences pattern with moderate sharp fall at the band edge, which is an indication of semiconductor behavior with good enough crystallinity. Figure 5 indicates that the transmission of 1, 2 and 3 Zn% molecular weight doped $CuInS_2$ films are higher than that of the undoped and the doped films with 4 Zn% molecular weight. This indicates that an increase in Zn doping content from a critical Zn% molecular weight value has great effect on the transmission properties. This value corresponds in this work to 2% Zn content value. We note also an improvement in sharp fall of the transmission at the band edge after annealing in particular for 2 and 3 Zn% molecular weight. This is an indication of good crystallinity which confirms the XRD results. In our case, as described elsewhere, the single source thermal evaporation method leads to $CuInS_2$ sulfur defect. Therefore, for lower Zn concentrations there is an improvement in crystallinity through occupying the sulfur site by the zinc and the $CuInS_2$ structure is not affected. Consequently, there is an improvement in transmission in near infrared spectral range and probably the sulfur vacancy sites (samples undoped) increase the absorption. It is clear that the transmission in the near infrared region decreases from 70% to 35% for the higher Zn-incorporation. We consider that the introduced Zn with high amount firstly compensates the sulfur vacancy sites after what the excess Zn atoms present an undesirable effect by decreasing the transmission in the near infrared spectral region. Although the detailed mechanism to explain the zinc effect in the decrease of the transmission is not clear yet.

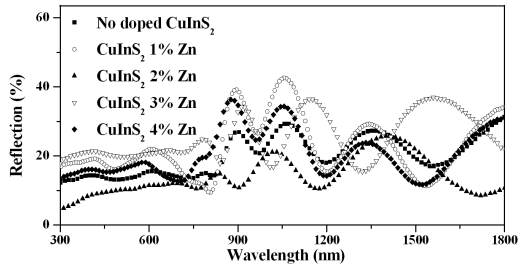

Fig. 4. Reflection spectra of undoped and Zn-doped $CuInS_2$ thin films with different Zn% molecular weight.

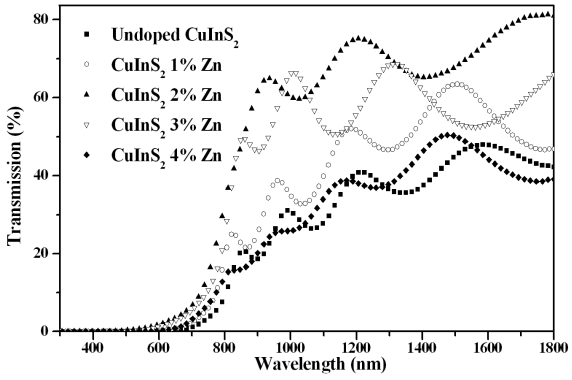

Fig. 5. Transmission spectra of undoped and Zn-doped $CuInS_2$ thin films with different Zn% molecular weight.

3.2.2. Absorption coefficients

The absorption coefficient (α) has been determined as a function of wavelength from measured reflectance R and transmittance T using the following equation [23, 24]:

$$\alpha = \frac{1}{d} \ln \left[\frac{(1-R)^2}{T} \right], \tag{3.2}$$

where d is the film thickness. Figure 6 shows the absorption coefficient versus the photon energy for the undoped and doped $CuInS_2$ thin films with 0 to 4 Zn% molecular weight after annealing in vacuum at 260°C for 2 h. It can be seen that all the films have relatively high absorption coefficients between 10^4 cm^{-1} and 10^5 cm^{-1} in the visible and the near-IR spectral range. Figure 6 clearly shows an improvement in the optical performance of $CuInS_2$ films doped with 3 Zn% molecular weight with sharp fall of the absorption at the band edge compared to that of the undoped or doped with other Zn content. This result is very important because we know that the spectral dependence of absorption coefficient affects the solar conversion efficiency [25].

3.2.3. Energy band gaps

In the high absorption region close to the beginning of band-to-band optical transmission (absorption coefficients $\alpha > 10^4$ cm^{-1}) the absorption is characterized by the following relation [26, 27]:

$$\alpha h\nu = A\left(h\nu - E_{\text{opt}}\right)^m, \tag{3.3}$$

where A is a constant, E_{opt} is the optical gap and m is an integer number which characterizes the transition process. Different authors [27–29] have suggested different

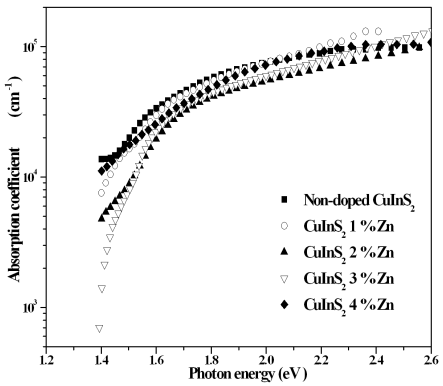

Fig. 6. Absorption coefficients spectra of undoped and Zn-doped $CuInS_2$ thin film with different Zn% molecular weight.

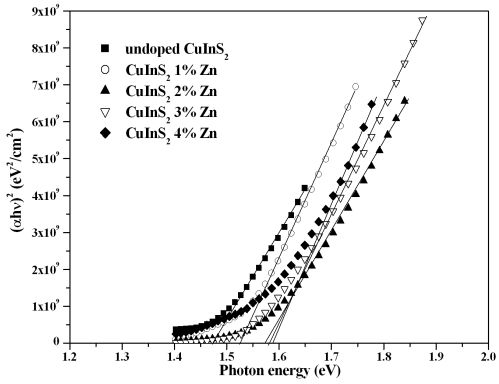

Fig. 7. Relationship between $(\alpha h\nu)^2$ and photon energy for undoped and Zn-doped $CuInS_2$ thin film with different Zn% molecular weight.

values of m for different glasses. The usual method for determining the values of E_{opt} involves plotting a graph of $(\alpha h\nu)^{1/m}$ vs. $h\nu$. An appropriate value of m is used to linearize the graph, the value of E_{opt} is given by the intercept on the $h\nu$ axis and the constant A can be determined from the slope. The best fit was found to be $m = 1/2$ which indicates that direct photon transition is involved (Fig. 7). It is now well established that $CuInS_2$ is a direct gap semiconductor [30–32], with the band extrema located at the center of the Brillouin zone. The absorption coefficient α is related to the energy gap E_{opt} according to the equation [33]:

$$(\alpha h\nu)^2 = A\,(h\nu - E_{\text{opt}})\,. \tag{3.4}$$

The direct band gap energy (Fig. 8) increased after annealing from 1.467 to 1.585 eV with increasing Zn content. We attribute this difference to the presence of an amorphous component and possibly the structural defects, since it cannot be excluded that the polycrystallinity of the films influences the optical absorption behavior and thus also the gap energy derived from the spectra. Also the amount of disorder in the material probably plays an important role in the optical band gap,

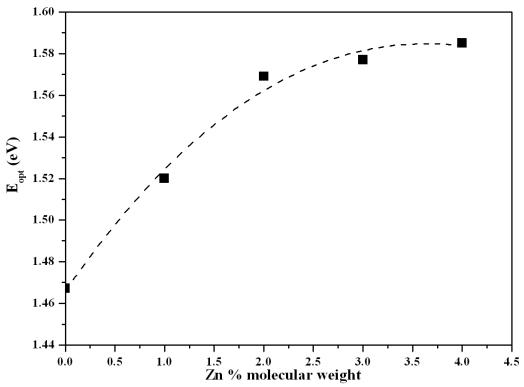

Fig. 8. Relationship between the optical bands gaps of $CuInS_2$/Zn with different Zn% molecular weight.

since the XRD analysis indicated that for the higher Zn% molecular weight a deterioration of the structural properties was observed which gives rise to defect states and thus induces smearing of absorption edge.

3.3. Electrical properties

Besides the optical properties, the electrical properties are also an important aspect of the performance of Zn doped $CuInS_2$ thin films. The effects of zinc doping on the electrical resistivity of $CuInS_2$ thin films were investigated. As-deposited and annealed undoped $CuInS_2$ thin films present higher resistivity values. The variations of the resistivity versus the Zn% molecular weight after annealing are shown in Fig. 9. The resistivity de-

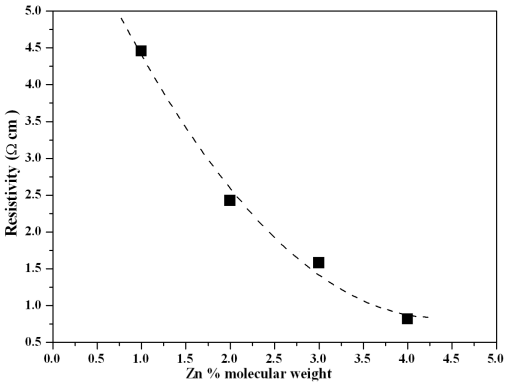

Fig. 9. Variations of the resistivity of Zn-doped $CuInS_2$ thin films with different Zn% molecular weight.

creases with increase in Zn content. It can be seen from Fig. 9 that the lowest electrical resistivity value of doped 4 Zn% molecular weight is 0.08 Ω cm with significant p-type conductivity. Therefore, how we can explain the p-conductivity in our case? It has been established by Ueng and Hwang [11] that in studying the defect structure of zinc-doped $CuInS_2$, we have to consider the basic defect states that would be formed by zinc in $CuInS_2$, crystals. They show that the incorporation of zinc in

$CuInS_2$ crystals can occur in three different ways, exclusively occupying the copper site to make a donor, occupying the sulfur site to make an acceptor and occupying the interstitial site to make a donor, and the donor Zn_{Cu} and Zn_i would be compensated by the acceptor Zn_S. It has been shown [22, 34] that the use of the single source thermal evaporation method to deposit $CuInS_2$ thin films leads to a deficit in sulfur. Consequently, it is probable that zinc in our case occupies the sulfur site to make an acceptor which can explain the origin of the *p*-type conductivity.

4. Conclusions

The effect of Zn doping on the structural and optical properties of $CuInS_2$ thin films has been investigated. Undoped and Zn-doped $CuInS_2$ thin films were grown by double source thermal evaporation. The films are annealed in vacuum for 2 h at 260°C. It was shown that Zn incorporation is possible and the control of Zn content is an important parameter to obtain Zn-doped $CuInS_2$ layers with high transmission. Moreover, up to 2 at.% Zn the transmission decreases. The absorption coefficients deduced from optical measurements are greater than 10^4 cm^{-1} in the range 1.4–2.6 eV after annealing. The direct band gap energy increased after annealing from 1.467 to 1.585 eV with increasing Zn% molecular weight. We attributed the higher values compared to that corresponding to the evaporated $CuInS_2$ thin films to the structural defects. The electrical resistivity of the Zn-doped $CuInS_2$ thin films decreases with increasing Zn content. The Zn-doped $CuInS_2$ thin films exhibit *p*-type conductivity explained by occupying the sulfur site by Zn species to make an acceptor.

References

[1] K. Ramanathan, M.A. Contreras, C.L. Perkins, S. Asher, S. Hasoon, J. Keane, D. Young, M. Romero, W. Metzger, R. Noufi, J. Ward, A. Duda, *Prog. Photovolt. Res. Appl.* **11**, 225 (2003).

[2] M.A. Contreras, K. Ramanathan, J. Abushama, F.S. Hasoon, D.L. Young, B. Egaas, R. Noufi, *Prog. Photovolt. Res. Appl.* **13**, 209 (2005).

[3] M.A. Contreras, B. Egaas, K. Ramanathan, G. Hiltner, A. Swartzlander, F. Hasoon, R. Noofi, *Prog. Photovolt.* **7**, 311 (1999).

[4] M. Powalla, B. Dimmler, R. Chaeffer, G. Woorwender, U. Stein, H.D. Mohring, F. Kessler, D. Hariskos, in: Proc. 19th *Europ. Photovoltaic Solar Energy Conf. and Exhibition, Paris (France) June 11–15, 2004*, p. 1663.

[5] R. Scheer, K. Diesner, H.-J. Lewerenz, *Thin Solid Films* **168**, 130 (1995).

[6] N. Meyer, I. Luck, U. Rühle, J. Klaer, R. Klenk, M.C. Lux-Steiner, R. Scheer, in: *Proc 19th Europ. Photovolaic Solar Energy Conf., Proc. Int. Conf., Paris (France) June 7–11, 2004*, p. 1698.

[7] K. Siemer, J. Klaer, I. Luck, J. Bruns, R. Klenk, D. Bräunig, *Solar Energy Mater Solar Cells* **67**, 159 (2001).

[8] G. Brandt, A. Ranber, J. Schneider, *Solid State Commun.* **12**, 481 (1983).

[9] J.J.M. Binsma, L.J. Giling, J. Bloem, *J. Lumirrex.* **27**, 35 (1982).

[10] S.D. Mittleman, R. Singh, *Solid State Commun.* **22**, 659 (1981).

[11] H.Y. Ueng, H.L. Hwang, *J. Phys. Chem. Solids* **51**, 11 (1990).

[12] T. Yamamoto, H.K. Yoshida, *Jpn. J. Appl. Phys.* **35**, L1562 (1996).

[13] T. Yamamoto, I.V. Luck, R. Scheer, *Appl. Surf. Sci.* **159-160**, 350 (2000).

[14] Y. Akaki, H. Komaki, H. Yokoyama, K. Yoshino, K. Maeda, T. Ikari, *J. Phys. Chem. Solids* **64**, 1863 (2003).

[15] M. Zribi, M. Kanzari, B. Rezig, *Europ. Phys. J. Appl. Phys.* **29**, 203 (2005).

[16] M. Ben Rabeh, M. Zribi, M. Kanzari, B. Rezig, *Mater. Lett.* **59**, 3164 (2005).

[17] M. Ben Rabeh, M. Kanzari, B. Rezig, *Thin Solid Films* **515**, 5943 (2007).

[18] T. Enzenhofer, T. Unold, R. Scheer, H.-W. Schock, in: *Material Research Society 2005 Spring Proc. San Francisco (CA) 2005, Spring Meeting*, MRS, 2005, p. F11.3.1.

[19] O.S. Heavens, *Optical Properties of Thin Solid Films*, Butterworths, London 1950.

[20] M. Kanzari, M. Abaab, B. Rezig, M. Brunel, *Mater. Res. Bull.* **32**, 1009 (1997).

[21] R. Scheer, K. Diesner, H.L. Lewerenz, *Thin Solid Films* **268**, 130 (1995).

[22] L.L. Kazmerski, G.A. Sanborn, *J. Appl. Phys.* **48**, 3178 (1977).

[23] D.E. Milovzorov, A.M. Ali, T. Inokuma, Y. Kurata, T. Suzuki, S. Hasegawa, *Thin Solid Films* **382**, 47 (2001).

[24] T.M. Wang, S.K. Zheng, W.C. Hao, C. Wang, *Surf. Coat. Technol.* **155**, 141 (2002).

[25] V.V. Kindyak, V.F. Gremenonok, I.V. Bodnar, V. Rud Yu, G.A. Madvedkin, *Thin Solid Films* **250**, 33 (1994).

[26] J. Tauc, R. Grigorovici, A. Vancu, *Phys. Status Solidi* **15**, 627 (1966).

[27] N.F. Mott, E.A. Davis, *Philos. Mag.* **22**, 903 (1970).

[28] E.A. Fagan, H. Fritzsche, *J. Non-Crystal. Solids* **2**, 80 (1970).

[29] K. Sedeek, M. Fadel, *Thin Solid Films* **229**, 223 (1993).

[30] B. Tell, J.L. Shay, H.M. Kasper, *Phys. Rev. B* **4**, 4455 (1971).

[31] H. Onnagawa, K.M. Miyashita, *J. Appl. Phys.* **23**, 965 (1985).

[32] N.N. Nishikawa, I. Aksenov, T. Sinzato, T. Sakamato, K. Sato, *Jpn. J. Appl. Phys.* **34**, L975 (1995).

[33] N.F. Mott, E.A. Davis, *Electronic Processes in Non--Crystalline Materials*, Clarendon Press, Oxford 1971.

[34] P. Migliorato, J.L. Shay, *J. Appl. Phys.* **46**, 1777 (1975).